Supplementary Table 1: Analysis of microarray-derived gene expression[1,2] for transcripts encoded within the 5 haplotype blocks (1-5, physical position on chromosome 3 shown in first column). Fold changes in expression with reference to WKY data are show along with Bonferroni-corrected *p* values. *Endog* was the only concordantly regulated and differentially expressed gene at the loci (---, no gene annotation).

			Fold change		P value	
Haplotype block	Probe ID	Gene symbol	SHR vs WKY	SHRSP vs WKY	SHR vs WKY	SHRSP vs WKY
1: 8870982-9022111	1388019_at	*Odf2*	-1.32	1.00	<0.05	n.s.
	1368466_a_at	*Odf2*	2.13	-1.00	<0.01	n.s.
	1399142_at	---	2.19	1.07	<0.0001	n.s.
	1393357_at	*Gle1*	-1.17	1.06	n.s.	n.s.
	1374690_at	*Gle1*	1.41	1.18	n.s.	n.s.
	1397752_at	---	-1.26	1.02	<0.01	n.s.
	1370838_s_at	*Spna2*	4.65	1.03	<0.0001	n.s.
	1379524_at	*Wdr34*	1.87	1.21	n.s.	n.s.
2: 9126115-9195508	1389642_at	---	3.11	-1.05	<0.01	n.s.
	1389816_at	***Endog***	**-1.75**	**-3.57**	**<0.01**	**<0.0001**
	1373782_a_at	*LOC499770*	-1.39	1.01	n.s.	n.s.
	1373667_at	*Ccbl1*	1.49	-1.51	<0.05	<0.05
3: 9815960-9980785	1393913_at	*RGD1311084*	-1.38	-1.00	n.s.	n.s.
	1381152_at	*Mettl11a*	1.88	-1.03	<0.01	n.s.
	1372185_at	*Mettl11a*	2.53	-1.23	<0.01	n.s.
	1371497_at	*Asb6*	1.56	1.06	n.s.	n.s.
	1390772_at	---	-1.21	1.03	n.s.	n.s.
	1374477_at	*Prrx2*	1.05	1.22	n.s.	n.s.
	1368015_at	*Ptges*	-2.29	-1.08	<0.01	n.s.
	1368014_at	*Ptges*	-3.96	-1.02	<0.0001	n.s.
4: 10039939-10197334	1378309_at	*Usp20*	1.52	1.07	n.s.	n.s.
	1376656_at	*Usp20*	1.85	-1.03	n.s.	n.s.
	1377941_at	---	-1.65	1.01	<0.0001	n.s.
	1376784_at	*Fnbp1*	-1.39	-1.10	n.s.	n.s.
	1372825_at	*Fnbp1*	2.51	-1.26	<0.0001	n.s.
	1373537_at	---	1.03	1.03	n.s.	n.s.
	1377342_s_at	*Fnbp1*	-1.72	1.06	<0.01	n.s.
	1390682_at	*Fnbp1*	-4.95	1.09	<0.0001	n.s.
	1369471_at	*Fnbp1*	1.12	1.18	n.s.	n.s.
	1395365_at	---	-1.54	1.09	n.s.	n.s.
	1379947_at	---	-2.13	1.05	<0.0001	n.s.
	1375406_s_at	*Fnbp1*	-1.62	-1.04	<0.05	n.s.
5: 10697268-10944869	1381483_at	---	-1.03	1.06	n.s.	n.s.
	1382390_at	---	-1.06	-1.08	n.s.	n.s.
	1393006_at	---	1.11	1.51	n.s.	n.s.
	1375614_at	*Prdm12*	-2.28	-1.04	<0.01	n.s.
	1379348_at	*Exosc2*	-1.05	1.04	n.s.	n.s.
	1371713_at	*Abl1*	2.84	-1.11	<0.01	n.s.
	1390677_at	*Fibcd1*	-1.12	-1.08	n.s.	n.s.

[1] Petretto, E. *et al.* Integrated genomic approaches implicate osteoglycin (Ogn) in the regulation of left ventricular mass. *Nat Genet* **40**, 546-552, (2008).

[2] Monti, J. *et al.* Soluble epoxide hydrolase is a susceptibility factor for heart failure in a rat model of human disease. *Nat Genet* **40**, 529-537, (2008).

Supplementary Table 2: Gene Ontology annotation of the sub-cellular localisation of the protein products of transcripts in the *ENDOG*-containing module. The module (Figure 3 of manuscript) was identified following topological overlap measure (TOM) analysis of transcripts from the GEO dataset GSE5406. Terms that remained significant following Bonferroni-correction are shown with an associated false discovery rate (FDR).

Term (Cellular component)	Count	Fold Enrichment	Bonferroni-corrected *p* value	FDR
GO:0005739~mitochondrion	70	9	2.35E-56	2.08E-55
GO:0005743~mitochondrial inner membrane	48	23	4.69E-52	4.15E-51
GO:0044429~mitochondrial part	57	14	9.12E-52	8.07E-51
GO:0019866~organelle inner membrane	48	21	1.73E-50	1.53E-49
GO:0005740~mitochondrial envelope	51	18	3.09E-50	2.74E-49
GO:0031966~mitochondrial membrane	50	19	6.07E-50	5.37E-49
GO:0044455~mitochondrial membrane part	34	40	2.81E-43	2.48E-42
GO:0031967~organelle envelope	51	12	1.53E-41	1.35E-40
GO:0031975~envelope	51	12	1.79E-41	1.59E-40
GO:0070469~respiratory chain	27	53	5.35E-37	4.73E-36
GO:0005746~mitochondrial respiratory chain	24	55	6.96E-33	6.16E-32
GO:0031090~organelle membrane	51	7	2.08E-29	1.84E-28
GO:0005747~mitochondrial respiratory chain complex I	20	70	3.32E-29	2.93E-28
GO:0045271~respiratory chain complex I	20	70	3.32E-29	2.93E-28
GO:0030964~NADH dehydrogenase complex	20	70	3.32E-29	2.93E-28
GO:0005753~mitochondrial proton-transporting ATP synthase complex	8	62	3.03E-09	2.68E-08
GO:0045259~proton-transporting ATP synthase complex	8	56	6.92E-09	6.12E-08
GO:0045263~proton-transporting ATP synthase complex, coupling factor F(o)	7	69	4.89E-08	4.33E-07
GO:0033177~proton-transporting two-sector ATPase complex, proton-transporting domain	7	43	1.25E-06	1.11E-05
GO:0016469~proton-transporting two-sector ATPase complex	8	26	2.37E-06	2.10E-05
GO:0005759~mitochondrial matrix	13	8	4.67E-06	4.13E-05
GO:0031980~mitochondrial lumen	13	8	4.67E-06	4.13E-05
GO:0000276~mitochondrial proton-transporting ATP synthase complex, coupling factor F(o)	4	65	3.16E-03	2.80E-02

Supplementary Table 3: Gene Ontology analysis of the biological processes associated with the *ENDOG*-containing module identified following topological overlap measure (TOM) analysis of transcripts from the GEO dataset GSE5406. Terms that remained significant following Bonferroni-correction ($p<0.05$) are shown with associated false discovery rates (FDRs).

Term (Biological process)	Count	Fold Enrichment	Bonferroni-corrected *p* value	FDR
GO:0006091~generation of precursor metabolites and energy	40	21	1.24E-39	3.34E-39
GO:0006119~oxidative phosphorylation	29	48	4.71E-38	1.27E-37
GO:0045333~cellular respiration	26	44	2.53E-32	6.82E-32
GO:0022900~electron transport chain	27	39	3.37E-32	9.09E-32
GO:0042775~mitochondrial ATP synthesis coupled electron transport	22	64	1.04E-30	2.79E-30
GO:0042773~ATP synthesis coupled electron transport	22	64	1.04E-30	2.79E-30
GO:0022904~respiratory electron transport chain	22	56	3.05E-29	8.22E-29
GO:0015980~energy derivation by oxidation of organic compounds	26	29	1.31E-27	3.54E-27
GO:0006120~mitochondrial electron transport, NADH to ubiquinone	19	74	2.80E-27	7.56E-27
GO:0055114~oxidation reduction	35	9	2.77E-21	7.47E-21
GO:0016310~phosphorylation	30	6	4.80E-13	1.29E-12
GO:0006793~phosphorus metabolic process	31	5	1.06E-11	2.84E-11
GO:0006796~phosphate metabolic process	31	5	1.06E-11	2.84E-11
GO:0015992~proton transport	7	19	9.47E-04	0.003
GO:0009060~aerobic respiration	6	28	0.001	0.003
GO:0006818~hydrogen transport	7	18	0.001	0.003
GO:0015986~ATP synthesis coupled proton transport	6	24	0.002	0.006
GO:0015985~energy coupled proton transport, down electrochemical gradient	6	24	0.002	0.006
GO:0034220~ion transmembrane transport	6	20	0.006	0.016
GO:0006754~ATP biosynthetic process	7	13	0.009	0.023
GO:0032981~mitochondrial respiratory chain complex I assembly	4	65	0.013	0.036
GO:0010257~NADH dehydrogenase complex assembly	4	65	0.013	0.036
GO:0009206~purine ribonucleoside triphosphate biosynthetic process	7	12	0.015	0.040
GO:0009145~purine nucleoside triphosphate biosynthetic process	7	12	0.016	0.043
GO:0009201~ribonucleoside triphosphate biosynthetic process	7	12	0.016	0.043
GO:0009142~nucleoside triphosphate biosynthetic process	7	11	0.019	0.051
GO:0046034~ATP metabolic process	7	11	0.022	0.060
GO:0033108~mitochondrial respiratory chain complex assembly	4	54	0.024	0.066
GO:0009152~purine ribonucleotide biosynthetic process	7	10	0.040	0.110
GO:0009205~purine ribonucleoside triphosphate metabolic process	7	10	0.040	0.110
GO:0009199~ribonucleoside triphosphate metabolic process	7	10	0.042	0.115

Supplementary Figure 1

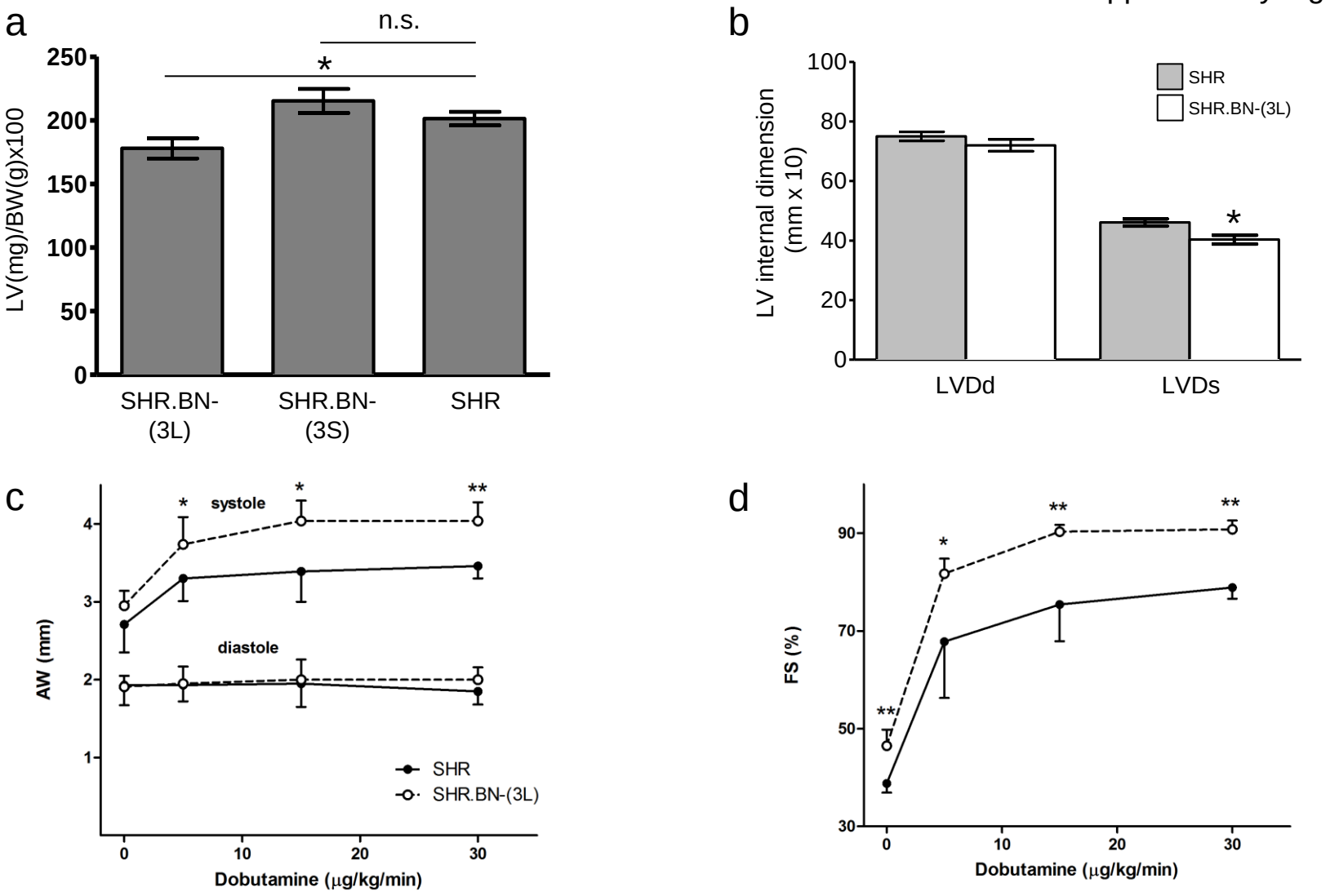

Supplementary Figure 1. SHR.BN-(3L) has lower LVM and better cardiac performance than the SHR. **a,** *Ex vivo* left ventricular weight (LV) normalised to body weight (BW); there was no difference in RV weight (data not shown). **b**, Left ventricular chamber dimension during diastole (LVDd) and systole (LVDs). **c and d** Dobutamine stress echocardiogram. **c,** Systolic and diastolic thickness of the LV anterior wall (AW) in response to increasing dobutamine dose. **d,** Fractional shortening (FS) of the LV in response to increasing dobutamine dose. Data are represented as means ±s.e.m. (a and b) and ±s.d. (c and d). *, $P<0.05$, **, $P<0.01$ (n ≥ 6 per genotype).

a

	Putative promoter		Exon I
	-313	-278	+454
SS/Jr	T	-	-
WKY/Tkyo	T	-	-
SHR/Tkyo	C	18 bp del	37 bp repeat
SHRSP/Tkyo	C	18 bp del	37 bp repeat

b

	Putative promoter		Exon I
	-313	-278	+454
WKY/NCrl	T	-	-
WKY/Ezo	T	-	-
WKY/Hcm	T	-	-
SHR/Ola	C	18 bp del	37 bp repeat
SHR/Hcm	C	-	37 bp repeat
SHR/Izm	C	18 bp del	37 bp repeat

c

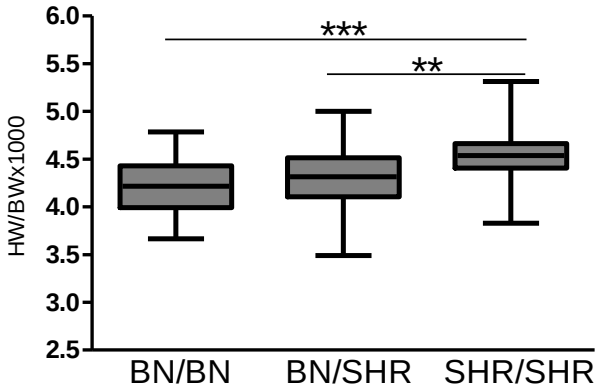

Supplementary Figure 2. ***Endog*** **sequence variants in rat strains and association of an exon 1 indel with HW**. **a**, Variants in rat strains used in previous studies to map the chromosome 3 LVM QTL. **b**, Variants in additional WKY and SHR sub-strains identifies an SHR-specific 37bp repeat in the SHR and SHR-derived strains. Numbering refers to nucleotide position relative to the transcription start site (TSS). The promoter was defined as the 2000 bps immediately upstream of the TSS. **c,** Association of the SHR-specific *Endog* indel with indexed HW in the BN x SHR F_2 population (box, inter-quartile range; line, median; whiskers, 5^{th}-95^{th} percentile).

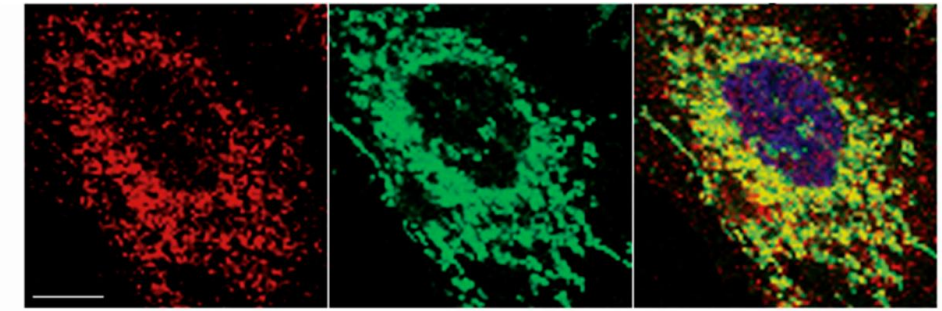

Supplementary Figure 3. Immunofluorescence confocal micrographs of Endog co-localisation with mitochondria in cardiomyocytes. Left, Endog labelled with a rabbit polyclonal antibody and Alexa568-conjugated secondary antibody; centre, mitochondria labelled with Mitotracker Green; right, merged image with co-localisation evidenced by yellow areas and nuclei counterstained with DAPI. Scale bar = 5 microns.

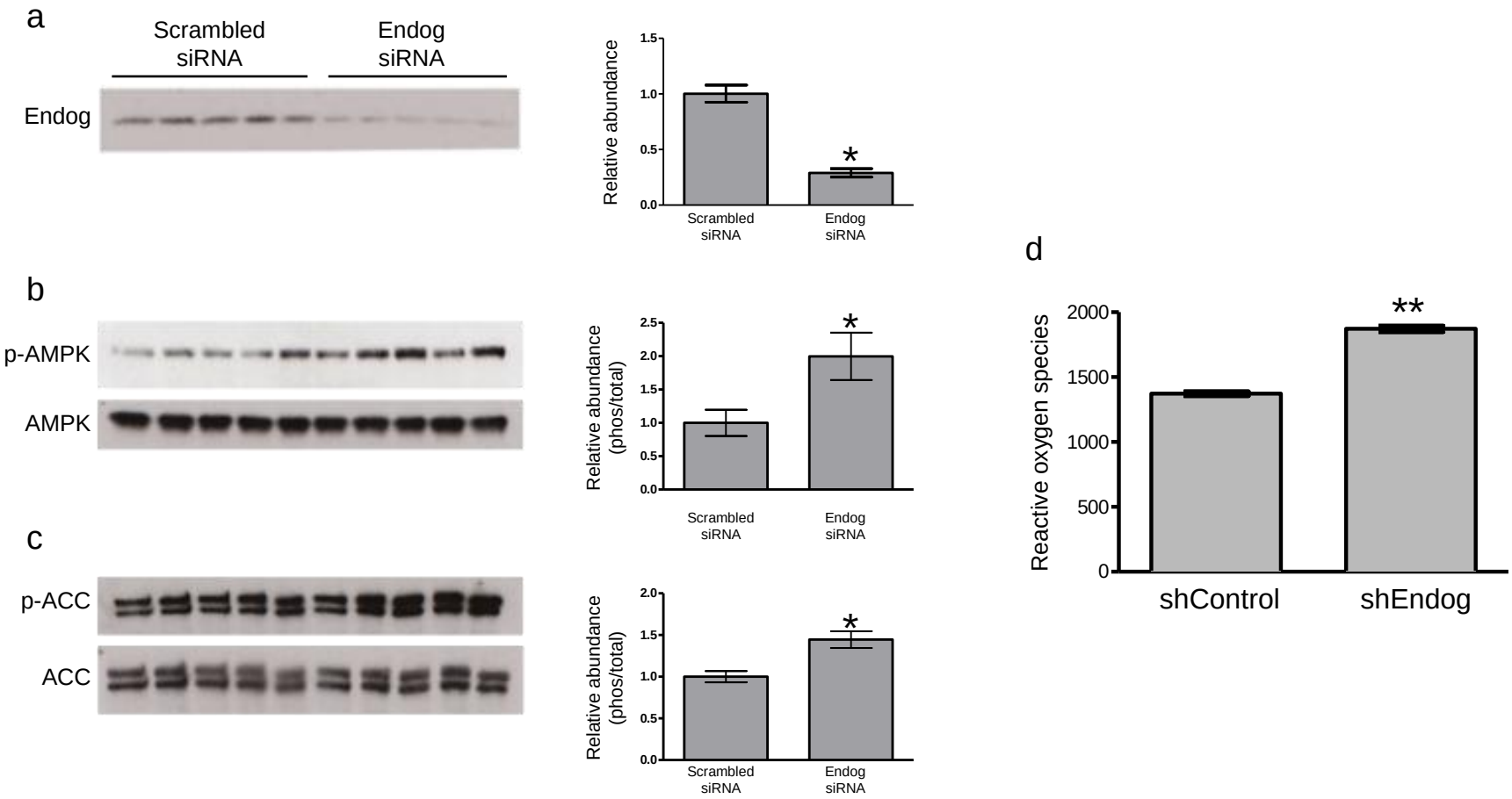

Supplementary Figure 4. Knockdown of *Endog* in primary cultures of neonatal rat ventricular cardiac myocytes activates AMPK with resultant ACC phosphorylation and induces reactive oxygen species (ROS) production. a, Immunoblot of Endog expression (left panel) and quantification of expression differences (right panel). **b,** Immunoblot of phospho-(Thr 172)-AMPK (p-AMPK) and total AMPK (left panel) and quantification of expression differences in p-AMPK normalised to total AMPK (right panel). **c,** Immunoblot of phospho-(Ser 79)-ACC (p-ACC) and total ACC (left panel) and quantification of expression differences in p-ACC normalised to total ACC (right panel). **a**-**c** Graphs, y axis units are arbitrary optical units. The experiment was repeated with similar results. **d**, Fluorescence-based quantification of ROS production in cardiomyocytes treated with shControl or sh*Endog.* Bars represent means±s.e.m. *, *P*<0.05, **, *P*<0.01.

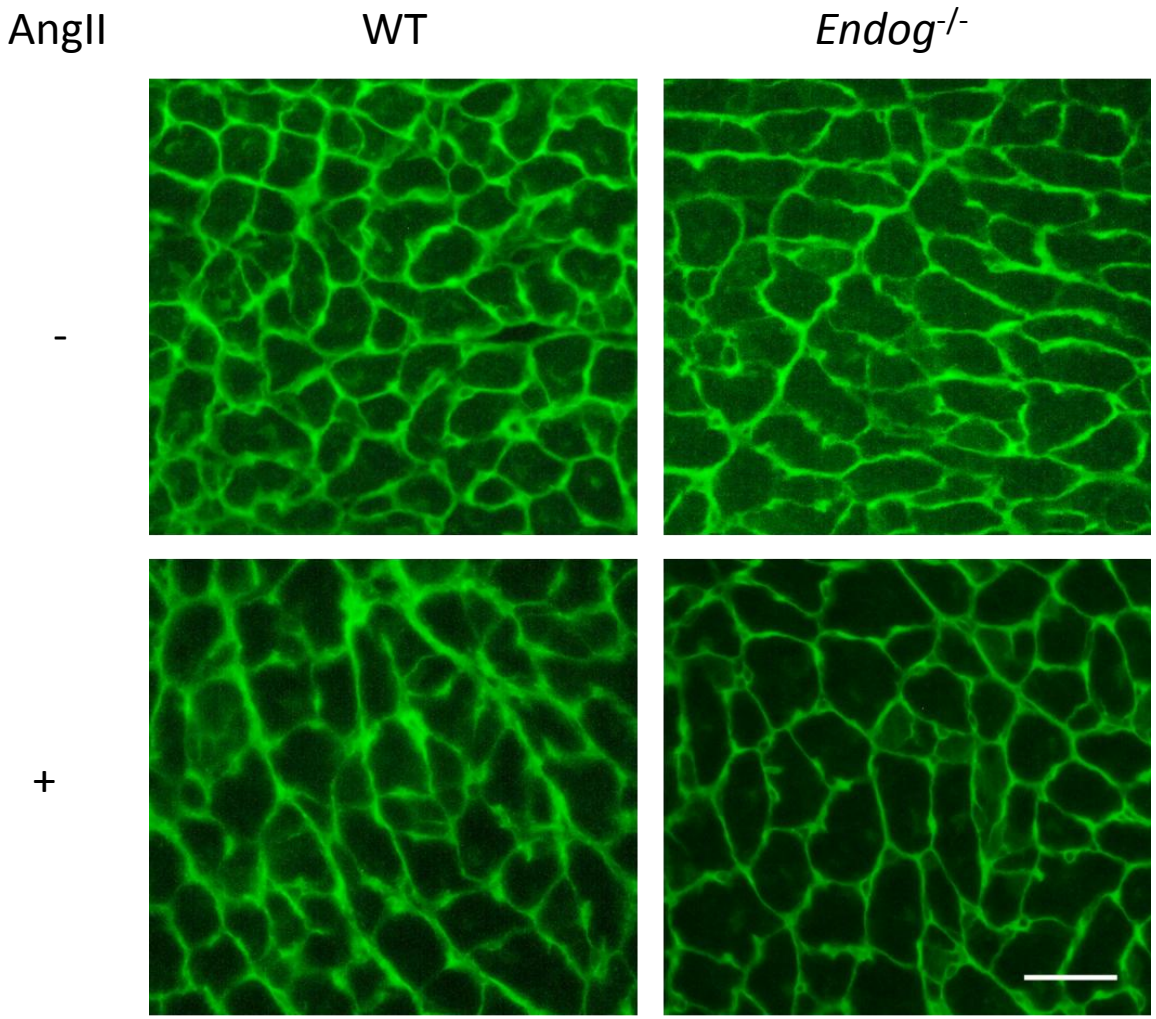

Supplementary figure 5. ***Endog*$^{-/-}$ mice have increased cardiomyocyte cross-sectional area at baseline and following angiotensin II (AngII) stimulation.** Representative fluorescence photomicrographs of left ventricular sections from *Endog*$^{-/-}$ and wildtype (WT) mice at baseline (-) and following AngII-induced hypertrophic stimulation (+). Sections were stained with WGA-FITC (10 µg/ml) to delineate the cell membrane. Scale bar: 50 microns.

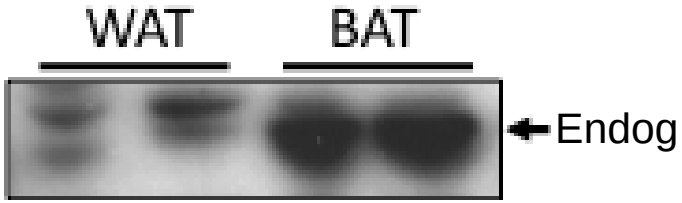

Supplementary figure 6. **Elevated Endog protein expression in brown adipose tissue**. Protein lysates from murine brown adipose tissue (BAT, n=2) and white adipose tissue (WAT, n=2) were analysed for Endog expression by immunoblotting. Equivalent loading was confirmed via Ponceau Red staining (not shown) (Endog: ~30kDa).

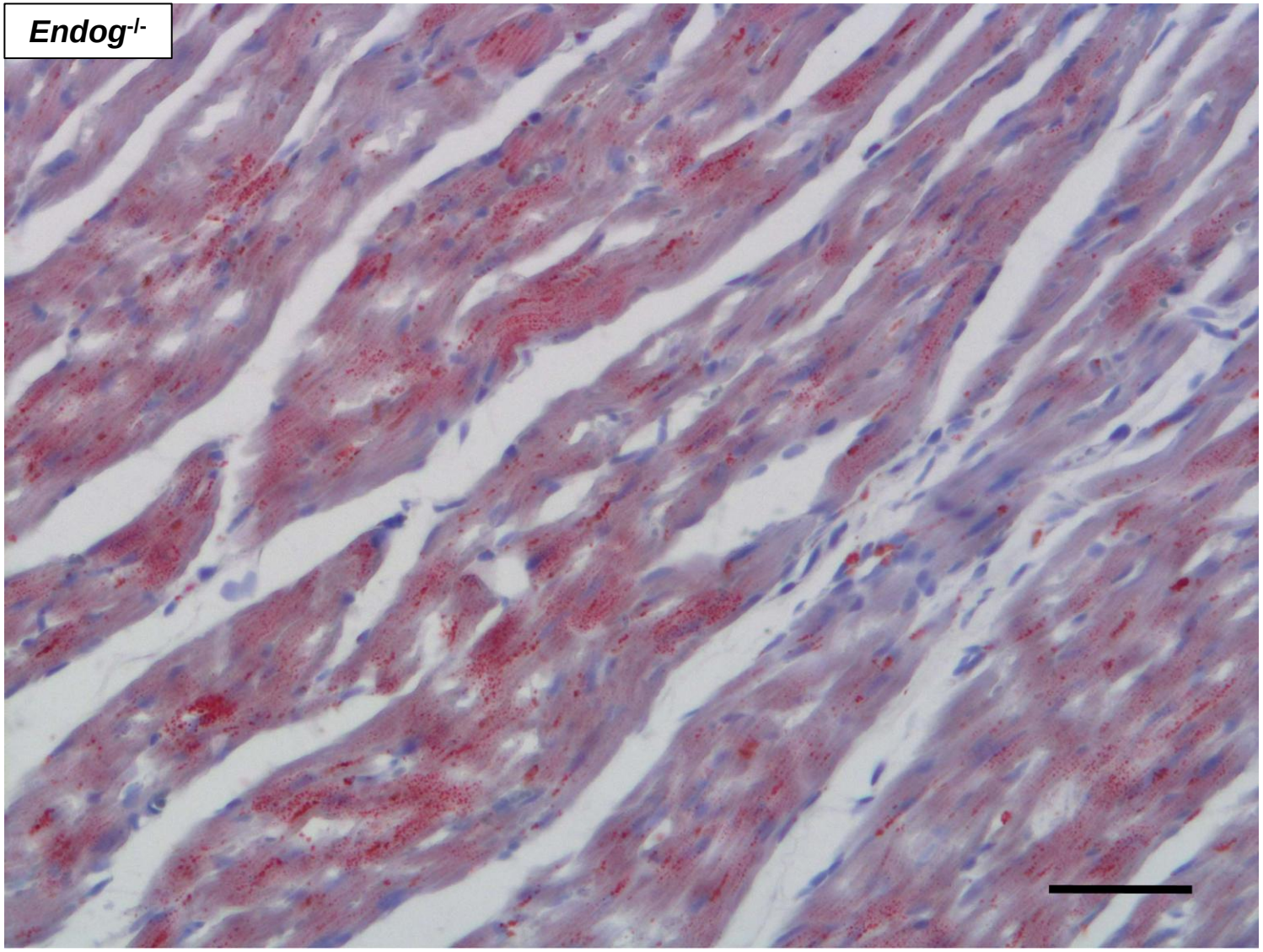

Supplementary Figure 7a. **High resolution oil red *O* staining for lipid in a left ventricular section from a 12-month old representative *Endog*$^{-/-}$ mouse (x40)**. Nuclei are stained with hematoxylin and appear blue. Scale bar=50 microns.

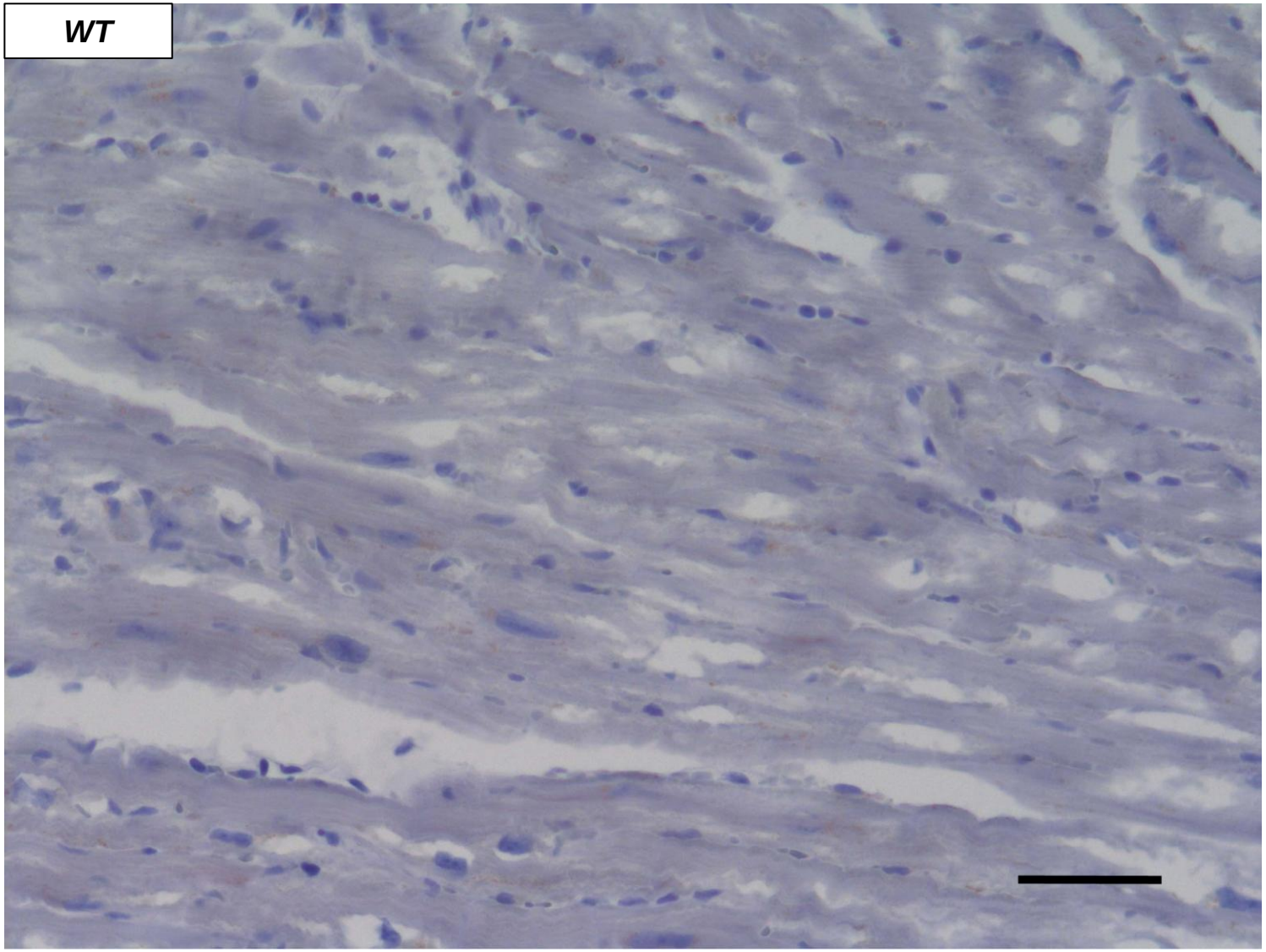

Supplementary Figure 7b. **High resolution oil red *O* staining for lipid in left a ventricular section from a 12-month old representative wildtype mouse (x40).** Nuclei are stained with hematoxylin and appear blue. Scale bar=50 microns.

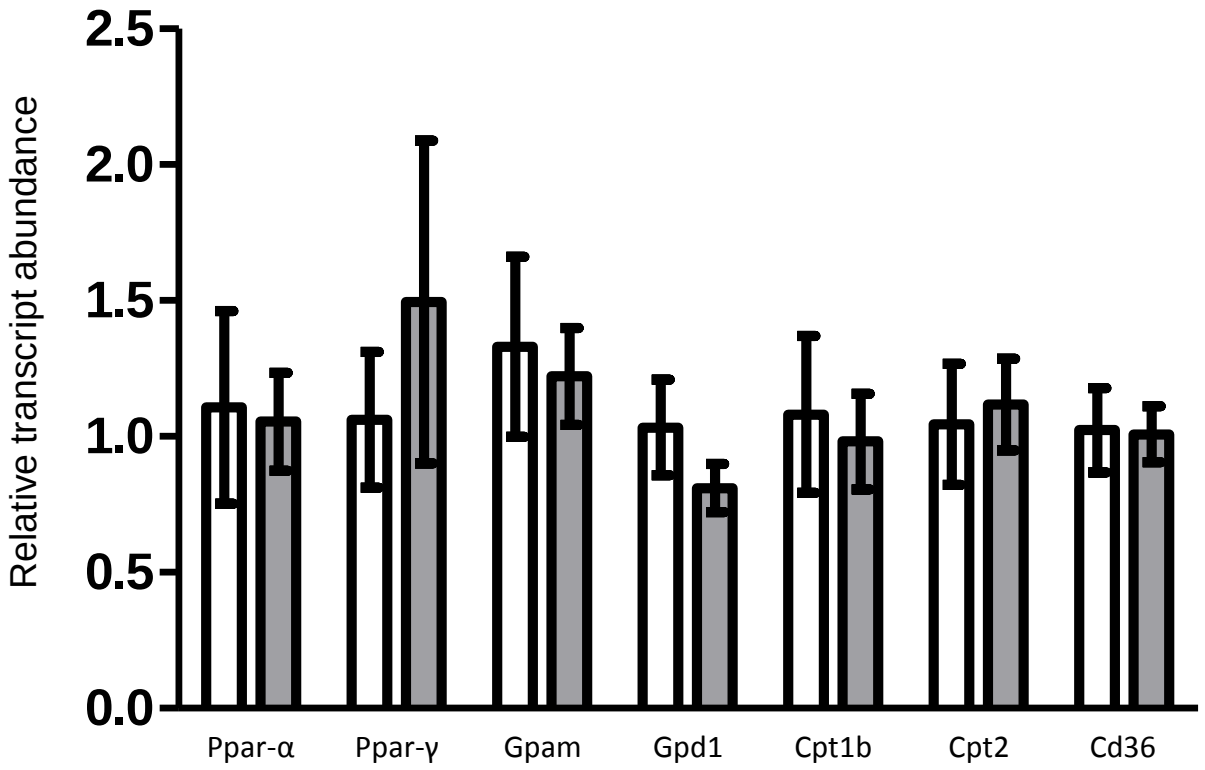

Supplementary Figure 8. **QPCR analysis of lipid metabolism genes in hearts of WT and *Endog*$^{-/-}$ mice (n=3)**. Data are presented as means ± s.e.m.

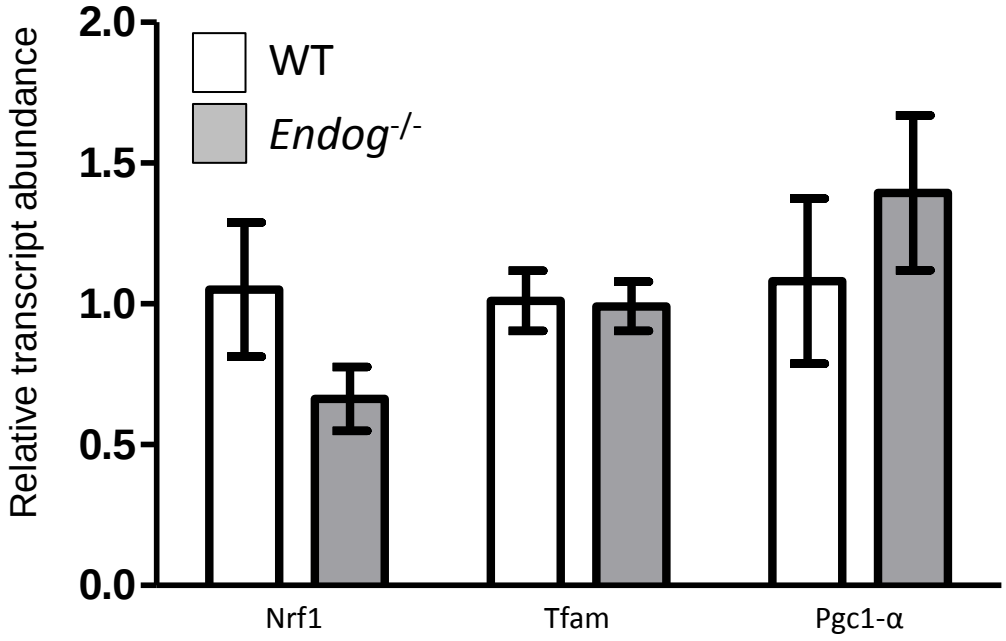

Supplementary Figure 9. **QPCR analysis of mitochondrial biogenesis genes in hearts of WT and *Endog*$^{-/-}$ mice (n=3)**. Data are presented as means ± s.e.m.

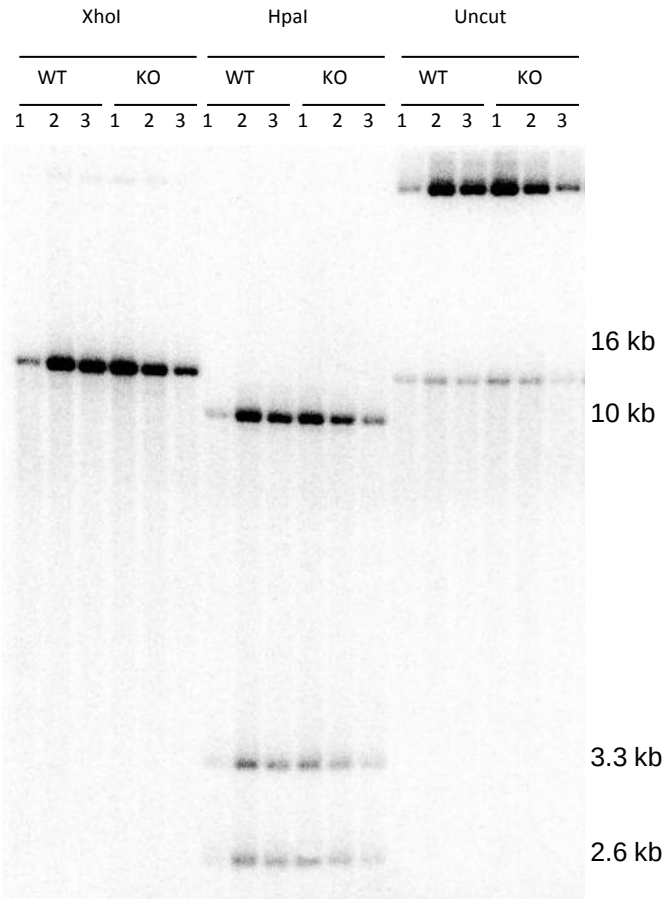

Supplementary Figure 10. Southern blot analysis of *Endog*$^{-/-}$ heart mitochondrial DNA. Total mtDNA from *Endog*$^{-/-}$ (n=3) and wildtype (n=3) mouse heart was digested with the indicated restriction enzymes before being electrophoresed on an agarose gel, transferred to a nylon membrane and incubated with a ^{32}P-labeled mouse mtDNA-specific probe (described in Supplementary Information). Values to the right denote fragment length in kilobases.

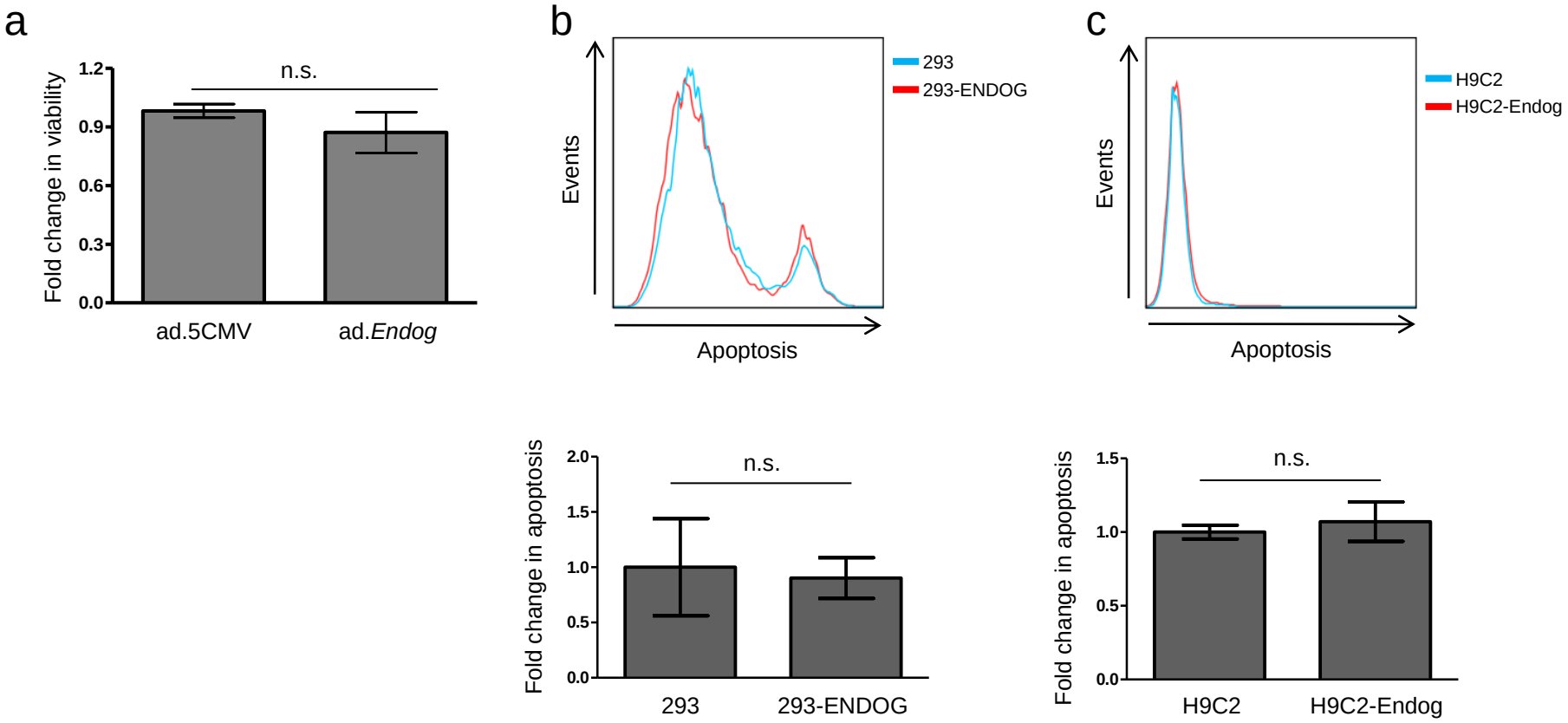

Supplementary Figure 11. **Acute and chronic over-expression of EndoG has no effect on apoptosis or necrosis.** (a) Myocytes were infected with ad.*Endog* (n=3) or a control virus at a concentration of 2 pfu/cell and cultured for 4 days to allow protein expression. Viability was assessed via spectrophotometric measurement of formazan (570 nm). (b) HEK293 cultures stably expressing *ENDOG* (n=3) were stained with AnnexinV and analysed by FACS. (c) H9C2 cells infected with ad.*Endog* (n=3) at a concentration of 2 pfu/cell were stained with AnnexinV and analysed by FACS. In **b** and **c**, top panels are histograms from one experiment and are representative of 3 biological replicates and bottom panels display mean AnnexinV signal±s.e.m and are expressed relative to control.